Structural analysis of strained p-type AlGaN/GaN superlattice

H. L. Tsai, T. Y. Wang, and J. R. Yang[a)]
Institute of Materials Science and Engineering, National Taiwan University, Taipei, Taiwan 106, Republic of China

C. C. Chuo and J. T. Hsu
Electronics and Optoelectronics Research Laboratories, Industrial Technology Research Institute, Hsinchu, Taiwan 310, Republic of China

M. Čeh
Department of Nanostructured Materials, Jožef Stefan Institute, 1000 Ljubljana, Slovenia

M. Shiojiri[b)]
Kyoto Institute of Technology, Kyoto 606-8585, Japan and Department of Anatomy, Kanazawa Medical University, Ishikawa 920-0293, Japan

(Received 22 September 2006; accepted 30 October 2006; published online 25 January 2007)

We investigated the nanostructure of AlGaN/GaN strained-layer superlattice (SLS) cladding in the GaN-based violet laser diode (LD) and the AlInGaN-based ultraviolet (UV) light emitting diode (LED) with a scanning transmission electron microscope (STEM). In the *p*-SLS cladding, comprising 34 pairs of p-$Al_{0.1}Ga_{0.9}N$/p-GaN:Mg layers in the GaN-based LD, the $Al_{0.1}Ga_{0.9}N$ and GaN layers were distinguished as dark and bright bands $\sim$6 nm wide in the high-angle annular dark-field (HAADF) STEM images. Threading dislocations (TDs) were observed. Among TDs that came from the underlying layer, some run outside through the SLS, and the others disappeared within the SLS, which discloses a role of the SLS in suppressing defect propagation. A HAADF-STEM image of the TD with a dark line along the center of a bright contour was found. The dark line, which was darker than the surrounding matrix, is striking. One of the probable explanations for the dark line that may be considered is local segregation of light atoms (Mg or Al) in Cottrell atmosphere around the dislocation core. In the HAADF-STEM image of the UV LED wafer, the AlInGaN and AlInGaN:Si layers in the MQW were definitely resolved, appearing as dark and bright bands. HAADF-STEM also distinguished between the AlGaN and GaN layers in the *p*-SLS cladding in the UV LED wafer. © *2007 American Institute of Physics*.
[DOI: 10.1063/1.2423142]

I. INTRODUCTION

Violet or purplish blue light emitting diodes (LEDs) and laser diodes (LDs) in the GaN-based multilayer system have been devised and widely manufactured. The active region of these devices is made of InGaN/GaN multiple quantum wells (MQWs).[1,2] The lifetime of the diodes, which exceeds 10 000 h,[3] is achieved by the epitaxial lateral overgrowth of the GaN contact layer on the sapphire substrate and the cladding of AlGaN/GaN strained-layer superlattices (SLSs). The epitaxial lateral growth greatly reduces the dislocation density in the GaN contact layer and consequently decreases lattice defects in its successive layers.[4,5] For optical confinement, the devices need thick AlGaN cladding layers on the GaN contact layers. However, the formation of the thick AlGaN cladding layers is impossible because cracks and dislocations are induced by lattice mismatching between the AlGaN and GaN. By using an AlGaN/GaN multilayer architecture, the formation of these defects is suppressed, thus allowing the growth of thick cladding layers.[3] Additionally, Mg-doped *p*-AlGaN/GaN SLSs have hole concentrations enhanced over 3×10^{18} cm^{-3} at room temperature, which exceeds more than ten times the value available in bulk AlGaN layers.[6,7] AlInGaN-based LEDs and LDs have lately attracted attention because of the emission wavelength covering a wide spectral range, from the visible spectrum to the ultraviolet (UV) region. A short wavelength of the stimulated emission of 328 nm in the UV region was achieved in $Al_{0.22}In_{0.02}Ga_{0.76}N/Al_{0.38}In_{0.01}Ga_{0.61}N$ MQW.[8]

The nanostructure of the SLS cladding greatly influences the final LED or LD properties. However, there have been very few structural investigations of the AlGaN/GaN SLS cladding. Saijo *et al.*[9] performed high-resolution (HR) field-emission gun scanning electron microscopy (FEG-SEM) observations of the SLS cladding layer using n-$Al_{0.14}Ga_{0.86}N$ (3 nm)/n-GaN (3 nm) layers. With the aid of image processing, the AlGaN and GaN layers were definitely resolved as bright and dark fringes in the mapping of secondary electrons. But the exact thickness of the layers could not be determined due to insufficient point-to-point resolution of the microscope. The backscattered electron images, however, did not distinguish between the $Al_{0.14}Ga_{0.86}N$ and GaN layers, because the mass difference between $Al_{0.14}Ga_{0.86}N$ and GaN is too small to identify them in the bulk specimen. The sec-

[a)]Author to whom correspondence should be addressed; electronic mail: jryang@ntu.edu.tw
[b)]Present address: 1-297 Wakiyama, Enmyoji, Kyoto 618-0091, Japan; electronic mail: shiojiri@pc4.so-net.ne.jp

 © 2007 American Institute of Physics

Downloaded 11 Sep 2008 to 140.112.113.225. Redistribution subject to AIP license or copyright; see http://jap.aip.org/jap/copyright.jsp

ondary emission yield greatly depends on the surface state of the materials so that the n-$Al_{0.14}Ga_{0.86}N$ and n-GaN layers might be distinguishable with each other in the secondary electron images. They also observed p-$Al_{0.14}Ga_{0.86}N/p$-GaN SLS cladding layer at the same imaging conditions. However, the contrast fringes were detected neither in the secondary electron images nor in the backscattered images. The difference in the secondary emission yields seems to be very small between p-$Al_{0.14}Ga_{0.86}N$ and p-GaN. Bremser *et al.*[10] and Pecz *et al.*[11] used transmission electron microscopy (TEM) to observe $Al_{0.2}Ga_{0.8}N/GaN$ and $Al_{0.06}Ga_{0.94}N/GaN$ layers. The layers could be observed in the diffraction contours caused by small strain fields along their interfaces. However, it was not possible to identify the AlGaN and GaN layers in the images or to evaluate their exact thickness. The AlGaN and GaN layers could not be distinguished even in the HRTEM image shown by Bremser *et al.*[10] Similarly, Shiojiri *et al.*[12] have demonstrated experimentally and in computer simulation that the $Al_{0.14}Ga_{0.86}N$ layers cannot be distinguished from the GaN layers in the HRTEM images.

Recently, Shiojiri *et al.*[12,13] have reported on high-angle annular dark-field (HAADF) scanning transmission electron microscopy (STEM) observations of n-$Al_{0.14}Ga_{0.86}N$ (3 nm) and n-GaN (3 nm) SLS cladding layers. HAADF-STEM has been widely used to characterize defects as well as to analyze perfect crystal structures.[14] HAADF-STEM imaging, mainly due to elastically scattered incoherent electrons or thermal diffuse scattering, gives rise to strong contrast dependence on the atomic number, unlike conventional TEM imaging due to elastically scattered coherent electrons. Therefore, HAADF-STEM enables us to acquire the chemical composition.[15,16] The $Al_{0.14}Ga_{0.86}N$ and GaN layers were distinguished as dark and bright bands in the HAADF images taken in the $[\bar{1}2\bar{1}0]$ zone axis.[12,13] The widths of the $Al_{0.14}Ga_{0.86}N$ and GaN layers were determined to be 2.24 ± 0.09 and 2.34 ± 0.15 nm, respectively, although they had nominally been deposited to be 3 nm. The lattice parameters of the $Al_{0.14}Ga_{0.86}N$ were evaluated to be $a=0.32\pm0.01$ nm and $c=0.50\pm0.02$ nm, and those of GaN were $a=0.32\pm0.02$ nm and $c=0.52\pm0.03$ nm. This was a direct illustration of the SLSs, where a good lattice matching in the basal plane caused by shrinkage of the $Al_{0.14}Ga_{0.86}N$ lattice normal to the basal plane suppresses the generation of misfit dislocations. Dislocations appeared as dark contours in bright-field STEM images and as bright contours in HAADF images. It was observed that threading dislocations reverted from running along the c direction to running in the basal plane. Since the converted dislocations would not reach the upper MQW layer, they could result in the overall reduction of structural defects in the active MQW layer.

In the present paper we show the structural and compositional analysis of the p-AlGaN/p-GaN SLSs with HAADF-STEM, since the p-AlGaN and p-GaN layers have not yet been distinguished in the SLS claddings.

II. EXPERIMENTAL PROCEDURE

We investigated p-SLSs in two specimens, which are schematically shown in Figs. 1(a) and 1(b). The heterostructures were grown by metal organic vapor-phase epitaxy (MOVPE) directly onto undoped GaN nucleation layer [low temperature GaN (LT-GaN)] that was previously deposited at a low temperature (550–570 °C) on the (0001) sapphire substrate. Specimen 1, shown in Fig. 1(a), is similar to the prototype wafer of the violet LD structure, as reported in previous papers.[17–19] Since this specimen was prepared to investigate details of the structure of the p-AlGaN/AlGaN SLS cladding layer, some underlying structures, including the n-AlGaN/AlGaN SLS cladding layer and the MQW layer, were not deposited. Specimen 2, shown in Fig. 1(b), is a wafer of UV LED, whose characteristics were reported by Wang *et al.*[20] In both of the specimens, the doped (Mg or Si) and undoped GaN layers, and the AlGaN/GaN SLSs and/or the doped AlGaN layers, were deposited at a high temperature (HT) (~1150 °C), and the multiple AlInGaN:Si/AlInGaN QW layer was deposited at 820 ~870 °C.

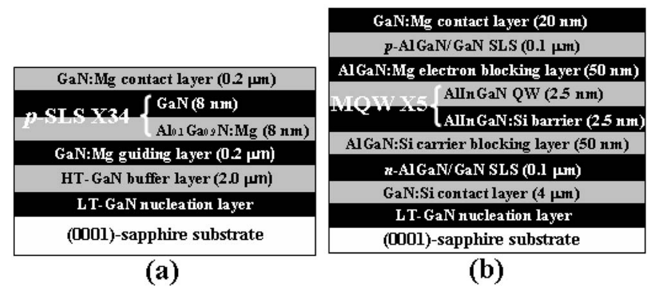

FIG. 1. Structure of the specimens observed in this experiment. (a) Specimen 1, which is a part of a standard GaN-based violet laser diode. (Ref. 17 and 18). The underlying n-type structures and the MQW were not deposited. The p-SLS cladding comprises 34 pairs of $Al_{0.1}Ga_{0.9}N:Mg$ layers and GaN layers. (b) Specimen 2, which is a wafer of ultraviolet LED (Ref. 20). The MQW comprises five pairs of $Al_{0.005}In_{0.02}Ga_{0.975}N$ QW layers and $Al_{0.12}In_{0.005}Ga_{0.875}N:Si$ barrier layers. The indicated value is a nominal thickness of each layer.

The specimens for HAADF-STEM and HRTEM were prepared by mechanical polishing, followed by Ar^+ ion milling at 5.0 kV for a short time within 60 s in a Gatan Model 691 precision ion polishing system (PIPS). HAADF-STEM and HRTEM observations were performed in a Tecnai 30, equipped with a lens of $C_s=1.2$ mm, operated at 300 keV. The HAADF-STEM images were recorded in a detector range of $D=36\sim181$ mrad using a convergent electron probe with a semiangle of $\alpha=15$ mrad. All the HAADF-STEM and HRTEM images presented in this paper are in their original form without any image processing.

III. RESULTS AND DISCUSSION

Figure 2 shows a HAADF-STEM image from specimen 1. The p-AlGaN/GaN SLS cladding layer is seen between the two GaN:Mg layers: the contact layer (left) and the guiding layer (right). The GaN:Mg guiding layer is not distinguished from the underlying HT-GaN buffer layer. Since the specimen thickness increased from the left to the right of the specimen, the HAADF-STEM intensity increased similarly as a whole.

Threading dislocations (TDs) in Fig. 2 appear as bright contours along the c direction. In HAADF-STEM images,

Downloaded 11 Sep 2008 to 140.112.113.225. Redistribution subject to AIP license or copyright; see http://jap.aip.org/jap/copyright.jsp

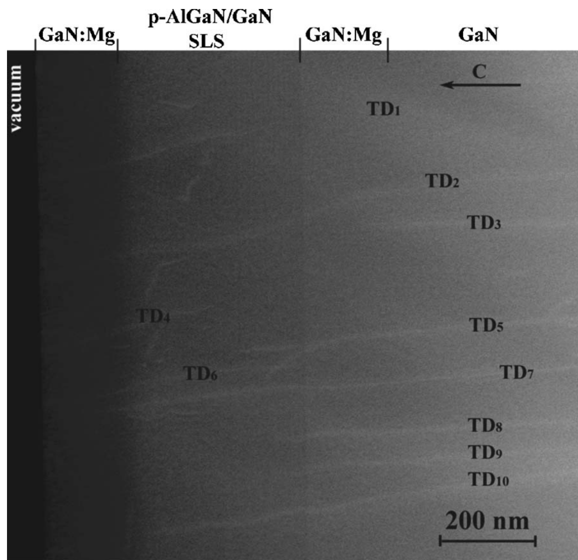

FIG. 2. HAADF-STEM image of specimen 1. The GaN:Mg contact layer, the p-AlGaN/GaN:Mg SLS cladding layer, the GaN:Mg guiding layer, and the underlying HT-GaN buffer layer are seen. Threading dislocations indicated by TD appear as bright contours along the c direction.

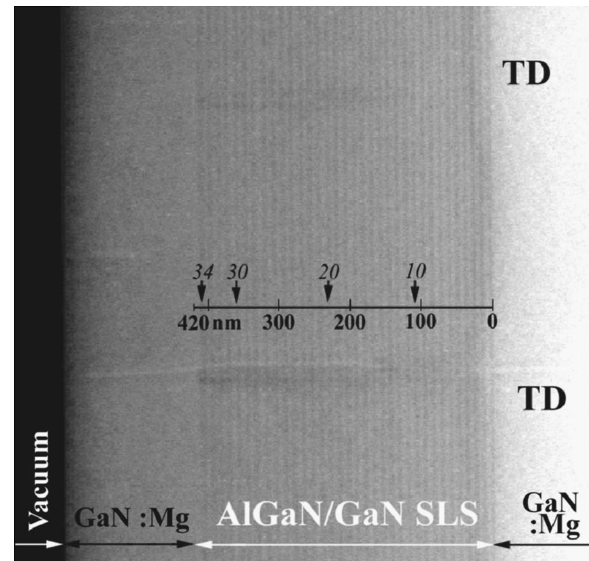

FIG. 3. HAADF-STEM image of the p-AlGaN/GaN:Mg SLS cladding. Thirty-four pairs of the $Al_{0.1}GaN_{0.9}N$ and GaN layer are seen, where the $Al_{0.1}Ga_{0.9}N$ and GaN layers appear as dark and bright bands. Threading dislocations are indicated by TD.

dislocations usually appear brighter than the matrix, which can be caused by static random displacement of atoms around defects.[14] The static displacement of atoms enhances diffuse scattering of electrons and contributes to the HAADF-STEM intensity, similar to thermal diffuse scattering, which is caused by thermally agitated random displacements of atoms. Therefore, HAADF-STEM imaging can more precisely locate the dislocations than diffraction contrast imaging in conventional TEM.

TDs are formed as a result of lattice mismatch between the epilayers. Most of them (for example, TD_1-TD_3 TD_5, TD_7-TD_{10} in Fig. 2) might be formed at the interface between the LT-GaN and the sapphire substrate. Among them, TD_1, TD_2, and TD_7 run outside through all the successive layers, while TD_3, TD_5 TD_8, TD_9, and TD_{10} stop and disappear at the interface between GaN:Mg layer and the SLS, or within the SLS. In a previous paper, Shiojiri *et al.*[12] found TDs reverted from running along the c direction to running in the basal plane in the n-$Al_{0.14}Ga_{0.86}N$ (3 nm) and n-GaN (3 nm) SLS cladding layers. Since the converted dislocations would not reach the upper MQW layer, this could result in the overall reduction of structural defects in the active MQW layer. The disappeared TDs in Fig. 2 are similar. The present observation gives a definite confirmation of an important role of the SLS in suppressing defect propagation (although the p-SLS cladding is an upper layer of the active MQW). However, TD_4 and TD_6 seem to be generated within the SLS cladding. Inquiry into more favorable conditions or precise control may be necessary in order to prevent the formation of TDs in the SLS layer.

Figure 3 shows a more greatly magnified HAADF-STEM image of the p-AlGaN/GaN SLS cladding. The cladding was prepared so as to comprise 34 pairs of the $Al_{0.1}GaN_{0.9}N$ and GaN layer. The image shows these 34 pairs as bright and dark bands parallel to the basal plane. According to the low thermal diffuse scattering cross section of Al atoms, the intensity of the $Al_{0.1}Ga_{0.9}N$ layers is weaker than that of GaN layers in the corresponding images. If the HAADF-STEM contrast is described as the Z contrast proportional to the square of the atomic number, the intensity ratio of $Al_{0.1}Ga_{0.9}N$ and GaN should be 90.7:100. Therefore, the dark bands correspond to the $Al_{0.1}Ga_{0.9}N$ layers, and the bright bands correspond to the GaN layers. This can be confirmed by the fact that the intensities of the GaN layers near both ends of the SLS exactly agree with those of the corresponding neighboring GaN:Mg layers. Previous papers[12] showed that HAADF-STEM distinguishes $Al_{0.14}Ga_{0.86}N$ layers from GaN layers in the n-SLS cladding, while the present experiment has shown that it can distinguish the $Al_{0.1}Ga_{0.9}N$ layers (having less Al content than 14%) from the GaN layer.

In the next step, we evaluated roughly the thickness of each layer. From the image in Fig. 3, the total thickness of the SLS cladding and the number of the pairs of AlGaN and GaN layers were measured to be 415 nm and 34, respectively, and thereby the average thickness of the pairs was estimated to be 12.2 nm. The image shown in Fig. 4 is from another area in the same SLS. From this image, the average thickness of the AlGaN and GaN pairs was estimated to be 138 nm/12=11.5 nm. Figure 5(a) is a HRTEM image of the same SLS. A dark band running vertically across the center is a diffraction contour of a threading dislocation. Thick horizontal dark or bright fringes indicate either AlGaN or GaN layers, respectively. The AlGaN layers and the GaN layers cannot be identified (in composition and region) from this HRTEM image. The (0001) lattice fringes in the AlGaN and GaN layers can be seen in Fig. 5(b), which is an enlarged image of the area framed in Fig. 5(a). We found 48 (0001) planes for a pair of the AlGaN and GaN layers, counting the number of lattice fringes. If we take that the AlGaN layers and the GaN layers have the same thickness and the same lattice constant c, we can assume the thickness of each AlGaN or GaN to be $=\sim 6$ nm and the lattice constants c of the

Downloaded 11 Sep 2008 to 140.112.113.225. Redistribution subject to AIP license or copyright; see http://jap.aip.org/jap/copyright.jsp

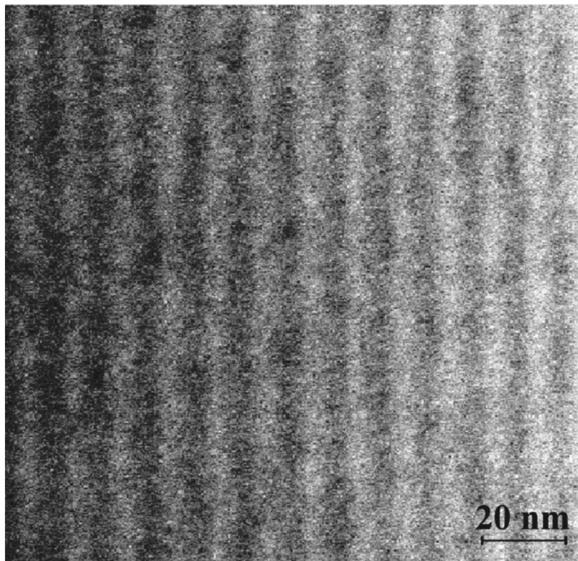

FIG. 4. HAADF-STEM image of the *p*-AlGaN/GaN:Mg SLS cladding. The $Al_{0.1}Ga_{0.9}N$ and GaN layers appear as dark and bright bands.

AlGaN and the GaN in the SLS cladding to be ~0.5 nm. The values of ~0.5 nm are reasonable, compared with values of 0.50 nm for $Al_{0.14}Ga_{0.86}N$ and 0.52 nm for GaN, which were precisely determined in the previous experiment.[12]

Figure 6 shows a HAADF-STEM image of the SLS cladding. Two TDs appear: one runs from the underlying layer to the outside through the SLS, and the other becomes extinct (like TD_3, TD_5 TD_8, TD_9, and TD_{10} in Fig. 2; reverting to running in the basal plane) in the SLS. If we examine in detail the image of each dislocation, we can find a dark line along the center of the bright contour. As mentioned above, the strong bright contour can be interpreted as coming from enhanced diffuse scattering that is ascribed to static displacement of atoms around the dislocation core.[12,14] The intensity of the striking dark line is weaker than that of the surrounding matrix. The intensity of thermal diffuse scattering is theoretically proportional to the square of the atomic number of each atom in the crystal. It is also proportional to the electron wave field in the crystal. The wave field is influenced by the lattice distortion, which is caused by substituted impurity atoms or a small tilt of zone axis with respect to the incident beam direction. Therefore, the contrast of dislocation in HAADF-STEM image cannot be interpreted exactly. Local segregation of light atoms (Mg or Al) in Cottrell atmosphere around the dislocation core may be a probable cause of the dark line.

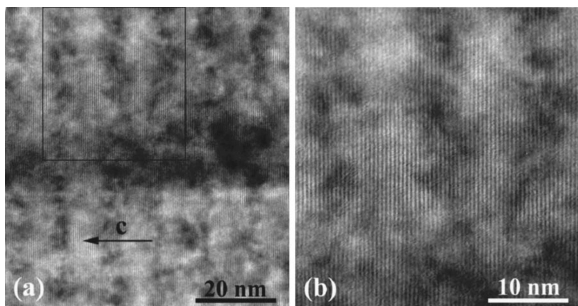

FIG. 5. (a) HRTEM image of the *p*-AlGaN/GaN:Mg SLS cladding. A threading dislocation runs vertically across the center. The lattice fringes corresponding to the (0001) atomic planes can be seen. (b) Enlarged image of the area framed in (a).

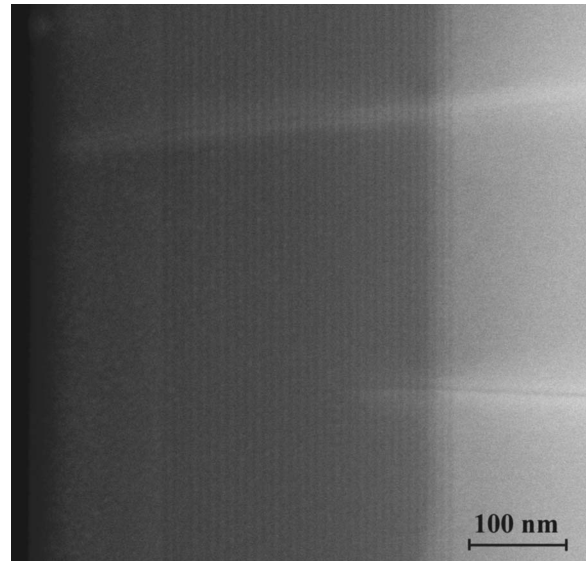

FIG. 6. HAADF-STEM image of the *p*-AlGaN/GaN:Mg SLS cladding. Two TDs appear. Each TD has a dark line along the center of the bright contour.

Recently, Shiojiri *et al.*[19] have discussed the formation mechanism of *V* defects, which are often observed nucleating on TDs crossed with the InGaN QW just above the GaN:Si underlying layer. The *V* defects have the thin six-walled structure with InGaN/GaN $\{10\bar{1}1\}$ QWs, which were found by HAADF-STEM (Ref. 21) and confirmed by backscattering electron images in FEG-SEM.[22] The formation of the *V* defect was explained by taking into account the growth kinetics of the GaN crystal and a masking effect of In atoms,[19] by analogy with the epitaxial lateral overgrowth.[4,5,23] That is, the growth rate of the $\{10\bar{1}1\}$ surface decreases if a temperature as low as 820–850 °C is used for the deposition of the InGaN/GaN QW layer. Then, if a mask disturbing the (0001) layer growth is formed, the termination would occur on the six $\{10\bar{1}1\}$ planes of the InGaN and GaN layers successively grown, which become the sidewalls of a V-shaped pit. Indium atoms trapped and segregated in the strained field around the core of a TD are suggested to play a role as a small mask, hindering Ga atoms from migrating on the (0001) monolayer to make a smooth (0001) monolayer. Thus, it should be noted that the generation of the *V* defects occurs at low reactor temperatures, at which the poor surface diffusion of Ga atoms and particularly In atoms impedes the layer-by-layer growth on the (0001) surface. This means that no *V* defects are generated in the structures grown at high temperature. The present observation has confirmed this mechanism, since we observed no *V* defects in the SLS cladding grown at 1150 °C on the GaN:Mg, as seen in Figs. 2–6.

Figure 7 shows a HAADF-STEM image of the UV LED wafer illustrated in Fig. 1(b). The GaN:Mg (20 nm) contact layer, the *p*-AlGaN/GaN (0.1 μm) SLS cladding layer, the AlGaN:Mg (50 nm) electron blocking layer, the AlInGaN (2.5 nm)/AlInGaN:Si (7.5 nm) MQW layer, the AlGaN:Si

Downloaded 11 Sep 2008 to 140.112.113.225. Redistribution subject to AIP license or copyright; see http://jap.aip.org/jap/copyright.jsp

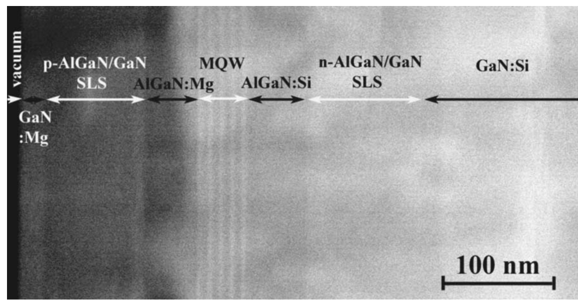

FIG. 7. HAADF-STEM image of the UV LED wafer illustrated in Fig. 1(b). The GaN:Mg (20 nm) contact layer, the p-AlGaN/GaN (0.1 μm) SLS cladding layer, the AlGaN:Mg (50 nm) electron blocking and capping layer, the AlInGaN (2.5 nm)/AlInGaN:Si (7.5 nm) MQW layer, the AlGaN:Si (50 nm) carrier blocking layer, the n-AlGaN/GaN (0.1 μm) SLS cladding layer, and a part of the GaN:Si (4 μm) contact layer were clearly distinguished. The $Al_{0.005}In_{0.02}Ga_{0.975}N$ QW layers and $Al_{0.12}In_{0.005}Ga_{0.875}N$:Si barrier layers in the MQW are definitely resolved, appearing as bright bands and dark bands, respectively.

(50 nm) carrier blocking layer, the n-AlGaN/GaN (0.1 μm) SLS cladding layer, and a part of the GaN:Si (4 μm) contact layer were clearly distinguished in this HAADF-STEM image, having thicknesses (shown in the brackets) as expected in the preparation. The AlInGaN layers and AlInGaN:Si layers in the MQW, which had been estimated to be comprised of $Al_{0.005}In_{0.02}Ga_{0.975}N$ QW layers and $Al_{0.12}In_{0.005}Ga_{0.875}N$:Si barrier layers,[20] are definitely resolved, appearing as bright bands and dark bands, respectively. A HAADF-STEM image in Fig. 8 shows the resolved AlGaN layers and GaN layers in the p-SLS cladding in the UV LD wafer. The Al composition of these AlGaN layers had been estimated as ~15%; that is, this p-SLS may be represented by p-$Al_{0.15}Ga_{0.85}N$/GaN.

IV. CONCLUSION

We investigated structural details of $Al_{0.1}Ga_{0.9}N$ and GaN:Mg layers in the p-SLS cladding and also an ultraviolet AlInGaN-based laser diode wafer with a scanning transmission electron microscope.

(1) The p-SLS cladding comprised 34 pairs of p-$Al_{0.1}Ga_{0.9}N$/p-GaN:Mg layers. The $Al_{0.1}Ga_{0.9}N$ layers and the GaN layers were distinguished as dark and bright bands, respectively, in HAADF-STEM images. The average thickness of the pair in the SLS was roughly estimated to be ~12 nm, which corresponds to 48 atom layers in the c direction. The estimated lattice constant c of the AlGaN and GaN in the SLS was approximately 0.5 nm, which is reasonable as compared with values of 0.50 nm for $Al_{0.14}Ga_{0.86}N$ and 0.52 nm for GaN in n-SLS cladding evaluated in a previous experiment.

(2) Threading dislocations (TDs) were observed. TDs formed in the underlying structures (such as the interface between the LT-GaN and the sapphire substrate) ran outside through the SLS and the upper layers or disappeared (reverted from running along the c direction to running in the basal plane) on the interface between the SLS/GaN:Mg or within the SLS. The disappearance of the TDs shows a role of the SLS in suppressing defect propagation. A few dislocations were formed within the SLS cladding. This may demand inquiry into more favorable conditions or precise control for the growth of the SLS layer.

(3) A HAADF-STEM image of a TD with a dark line along the center of the bright contour was found. The strong bright contour is interpreted to be caused by enhanced diffuse scattering that is ascribed to static displacement of atoms around the dislocation core.[14] The dark line, which was darker than the surrounding matrix, is striking. One probable explanation for the dark line may be local segregation of light atoms (Mg or Al) in Cottrell atmosphere around the dislocation core.

(4) No V defects were observed in the SLS. This is ascribed to a high reactor temperature of 1150 °C at which the SLS layer was deposited.

(5) HAADF-STEM clearly distinguished between the GaN:Mg contact layer, the p-AlGaN/GaN SLS cladding layer, the AlGaN:Mg cap and electron blocking layer, the AlInGaN/AlInGa:Si MQW layer, the AlGaN:Si carrier blocking layer, the n-AlGaN/GaN SLS cladding layer, and the GaN:Si contact layer, showing each layer to have the thickness expected in the preparation. The $Al_{0.005}In_{0.02}Ga_{0.975}N$ QW layers, which were 2.5 nm thick, and the $Al_{0.12}In_{0.005}Ga_{0.875}N$:Si barrier layers, which were 7.5 nm thick, in the MQW were definitely resolved, appearing as bright bands and dark bands, respectively. HAADF-STEM also distinguished between the AlGaN layers and the GaN layers in the p-SLS cladding in the UV LED wafer.

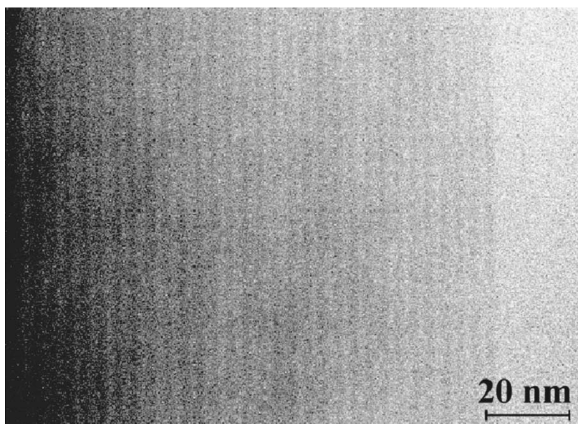

FIG. 8. HAADF-STEM image of the p-AlGaN/GaN SLS cladding in the UV LED wafer. The AlGaN layers and GaN layers appear as dark and bright bands.

HAADF-STEM imaging contrast depends directly on the composition of the layers. Distinguishing between p-AlGaN and p-GaN layers, which FEG-SEM previously failed in,[9] was achieved by HAADF-STEM. Functional devices, such as quantum well lasers, tunneling devices, random access memories, and high electron mobility transistors, usually comprise nanoscale multilayer heterostructures that exploit quantum confinement effects. Since the *in situ* monitoring in most processing equipment is still absent, atomic-scale analysis is required for understanding the real structure

Downloaded 11 Sep 2008 to 140.112.113.225. Redistribution subject to AIP license or copyright; see http://jap.aip.org/jap/copyright.jsp

in the final product, including the thickness and the composition of each layer. Only then can improvement of the functional properties and control of the product's quality be carried out. HAAD-STEM has become one of the most powerful analytical tools for characterization of these nanostructures.

ACKNOWLEDGMENTS

We thank T. C. Wang and Z.-H. Lee for assistance in MOCVD growth, which was financially supported by the Ministry of Economic Affairs of Taiwan, R.O.C., Project No. 5351AA4110.

[1] I. Akasaki, H. Amano, S. Sota, H. Sakai, T. Tanaka, and M. Koike, Electron. Lett. **32**, 1105 (1996).
[2] S. Nakamura, M. Senoh, S. Nagahara, N. Iwasa, S. Saito, T. Matsushita, Y. Sugimoto, and H. Kiyoku, Appl. Phys. Lett. **69**, 4056 (1996).
[3] S. Nakamura *et al.*, Appl. Phys. Lett. **72**, 211 (1998).
[4] A. Usui, H. Sunakawa, A. Sakai, and A. Yamaguchi, Jpn. J. Appl. Phys., Part 2 **36**, L899 (1997).
[5] O. H. Nam, M. D. Bremser, T. Zheleva, and R. Davis, Appl. Phys. Lett. **71**, 2638 (1997).
[6] K. Kumakura, T. Makimoto, and N. Kobayashi, Jpn. J. Appl. Phys., Part 1 **39**, 2428 (2000).
[7] P. Kozodoy, M. Hansen, S. P. DenBaars, U. K. Mishra, and J. Kauffman, Appl. Phys. Lett. **74**, 3681 (1999).
[8] K. Kazlauskas *et al.*, Mater. Sci. **7**, 209 (2001).
[9] H. Saijo, M. Nakagawa, M. Yamada, J. T. Hsu, R. C. Tu, J. R. Yang, and M. Shiojiri, Jpn. J. Appl. Phys., Part 1 **43**, 968 (2004).
[10] M. D. Bremser, W. G. Perry, T. Zheleva, N. V. Edwards, Q. H. Nam, N. Parikh, D. E. Aspnes, and R. F. Davis, MRS Internet J. Nitride Semicond. Res. **1**, 8 (1996).
[11] B. Pecz, Zs. Makkai, M. A. di Forte-Poisson, F. Huet, and R. E. Dunin-Borkowski, Appl. Phys. Lett. **78**, 1529 (2001).
[12] M. Shiojiri, M. Čeh, S. Šturm, C. C. Chuo, J. T. Hsu, J. R. Yang, and H. Saijo, J. Appl. Phys. **100**, 013110 (2006).
[13] M. Shiojiri, M. Čeh, S. Šturm, C. C. Chuo, J. T. Hsu, J. R. Yang, and H. Saijo, Appl. Phys. Lett. **87**, 031914 (2005).
[14] S. J. Pennycook and P. D. Nellist, in *Impact of Electron and Scanning Probe Microscopy on Materials Research*, edited by D. G. Rickerby, G. Valdre, and U. Valdre (Kluwer Academic, Dordrecht, 1999), pp.161–207.
[15] M. Kawasaki, T. Yamazaki, S. Sato, K. Watanabe, and M. Shiojiri, Philos. Mag. A **81**, 245 (2001).
[16] T. Yamazaki, K. Watanabe, Y. Kikuchi, M. Kawasaki, I. Hashimoto, and M. Shiojiri, Phys. Rev. B **61**, 13833 (2000).
[17] R. C. Tu, W. H. Kuo, T. C. Wang, C. J. Tun, F. C. Hwang, J. Y. Chi, and J. T. Hsu, Proceedings of the Fourth International Symposium on Blue Laser and Light Emitting Diodes, Cordoba, Spain, 2002 (unpublished), p. 1.
[18] R. C. Tu *et al.*, IEEE Electron Device Lett. **24**, 206 (2003).
[19] M. Shiojiri, C. C. Chuo, J. T. Hsu, J. R. Yang, and H. Saijo, J. Appl. Phys. **99**, 073505 (2006).
[20] T. C. Wang, H. C. Kuo, Z. H. Lee, C. C. Chuo, M. Y. Tsai, C. E. Tsai, T. D. Lee, and J. Chi, J. Cryst. Growth **287**, 582 (2006).
[21] K. Watanabe *et al.*, Appl. Phys. Lett. **82**, 718 (2003).
[22] H. Saijo, J. T. Hsu, R. C. Tu, M. Yamada, M. Nakagawa, J. R. Yang, and M. Shiojiri, Appl. Phys. Lett. **84**, 2271 (2004).
[23] K. Hiramatsu, K. Nishiyama, A. Motogaito, H. Miyake, Y. Iyechika, and T. Maeda, Phys. Status Solidi A **176**, 535 (1999).

Downloaded 11 Sep 2008 to 140.112.113.225. Redistribution subject to AIP license or copyright; see http://jap.aip.org/jap/copyright.jsp